J. Fluid Mech. (1965), *vol.* 23, *part* 2, *pp.* 229–240
Printed in Great Britain

Experimental study of the impingement of a liquid jet on the surface of a heavier liquid

By ROBERT B. BANKS† AND ANUSORNANT BHAVAMAI‡
SEATO Graduate School of Engineering, Bangkok, Thailand

(Received 15 March 1964 and in revised form 1 February 1965)

This study is concerned with the phenomenon of a liquid jet impinging normally on the surface of a heavier immiscible liquid. In essence, the work is a continuation of a previous investigation which involved an air jet impinging on a water surface.

An analytical model is presented which relates the velocity of the jet in the neighbourhood of the interface to the depth of cavity created by the jet. The effect of interfacial tension is taken into account. Numerous experiments were conducted utilizing both circular and plane jets. An oil jet impinging on water and a water jet impinging on carbon tetrachloride were studied. The resulting experimental data were analysed in terms of the dimensionless quantities obtained from the analytical model.

Results obtained from the circular-jet experiments were in close agreement with the results of the previously conducted air-water tests. However, there were some discrepancies in the plane-jet results; side-wall boundary-layer effects may be the explanation. Depending on the relative values of the Froude and Weber numbers, interfacial tension may be important in determining the depth of cavity created by a jet. Finally two intriguing phenomena, viz. interfacial shearing and cavity oscillation, were observed in the plane-jet experiments.

1. Introduction

In an earlier study, Banks & Chandrasekhara (1963) carried out an experimental investigation of the phenomenon of an air jet impinging on or penetrating through a water surface. Both 'free streamline' and turbulent spreading jets were considered and both circular and plane jets were investigated. Only the case of right-angle impingement was studied.

Two analytical models were devised to provide a framework for the analysis of experimental data. The first, a stagnation-pressure analysis, related the depth of the surface depression or cavity to the centre-line velocity of the jet in the proximity of the surface. The second, a displaced-liquid analysis, related the weight of the liquid displaced from the cavity to the jet momentum.

In this previous study, nearly 300 experiments were conducted in which broad ranges of the pertinent independent variables were covered. The depth of the surface depression or cavity was the most relevant dependent variable,

† Now at the University of Illinois at Chicago Circle.
‡ Now at the Department of Public and Municipal Works, Bangkok.

though cavity diameters or widths and cavity-lip heights also were measured. Experimental data were computed in terms of the dimensionless quantities obtained from the analytical models. Reasonably consistent dimensionless plots for all experimental data were the main results.

Recently there have been several studies devoted to ramifications of the above-described phenomenon. For example, Maatsch (1962) conducted experiments on the penetration of oxygen and carbon dioxide jets in water, oil, zinc chloride solution, and molten tin. Banks (1962) investigated the problem of a vertical plane gas jet impinging on a horizontally moving liquid. Olmstead & Raynor (1964) carried out the analytical solution of a plane free-streamline jet impinging on a deformable surface.

The present study is devoted to the phenomenon of a liquid jet impinging on the surface of a heavier immiscible liquid. Pertinent fluid properties and dimensions are defined in figure 1.

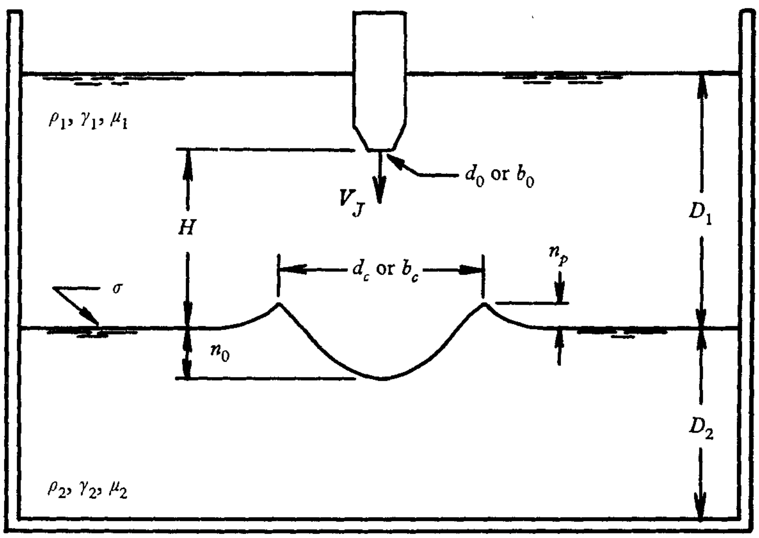

FIGURE 1. Definition sketch for the jet impingement study.

2. Analytical models of the impinging jet

2.1. *The circular jet*

Consider a liquid jet of density, ρ_1, discharging from a nozzle of diameter d_0, at a velocity, V_J. The nozzle is located a distance H above an otherwise quiescent interface between two immiscible liquids. The upper liquid is the same as the jet liquid. The lower liquid has a density ρ_2, and the interfacial tension is σ. A depression or cavity of maximum depth, n_0, is created at the interface by the jet. In addition, a cavity diameter d_c and cavity lip height n_p appear as a result of the impinging jet.

For values of H/d_0 less than about six, the jet behaves as a free streamline jet, i.e. no spreading occurs. In this instance, the centre-line velocity V_0 at some distance above the stagnation point is simply V_J. For larger values of H/d_0, the centre-line velocity decreases as a result of spreading. For this case, it is assumed that $V_0 = K_2(d_0/H)V_J$ in the neighbourhood of the stagnation point. The value of K_2 is about 6·5, as determined by several previous investigators, e.g. Corrsin & Uberoi (1949).

The condition for equilibrium at the stagnation point is

$$\tfrac{1}{2}\rho_1 V_0^2 + \gamma_1 n_0 = \gamma_2 n_0 + 2\sigma/R_0, \tag{2.1}$$

where R_0 is the radius of curvature of the interface at the stagnation point and $\gamma = \rho g$ is the specific weight of the respective liquids.

In the light of results obtained previously by Banks & Chandrasekhara, it is assumed that the shape of the interfacial depression is approximated by a normal-error curve. For large values of H/d_0, the cavity profile, $n = n(r)$, is assumed to be

$$n/n_0 = \exp\{-\beta_*(r/H)^2\}. \tag{2.2}$$

In the previous study, a value of $\beta_* = 125$ was obtained. Employing (2.2) to compute R_0, one obtains from (2.1)

$$\frac{n_0}{H}\left\{1+\frac{4\beta_*\sigma}{(\gamma_2-\gamma_1)H^2}\right\}^{-\frac{1}{2}} = \left\{\frac{\pi}{2K_2^2}\right\}^{\frac{1}{2}}\left\{\frac{M}{(\gamma_2-\gamma_1)n_0^3}\right\}^{-\frac{1}{2}}, \tag{2.3}$$

in which $M = \frac{1}{4}\pi\rho_1 d_0^2 V_J^2$. The above expression is identical to that presented in figure 11 of the previous paper (Banks & Chandrasekhara 1963) except that γ is now replaced by $(\gamma_2 - \gamma_1)$.

2.2. *The plane jet*

A similar analysis is made for the case of a plane jet discharging from a nozzle of width b_0 and length L. For small values of H/b_0, the centre-plane velocity, V_0, in the neighbourhood of the stagnation point is equal to V_J. For large values of H/b_0, the centre-plane velocity is approximately $V_0 = K_1(b_0/H)^{\frac{1}{2}}V_J$. Previous investigators have determined that K_1 has a value of about 2·5.

For a plane cavity, stagnation-point equilibrium requires that

$$\tfrac{1}{2}\rho_1 V_0^2 + \gamma_1 n_0 = \gamma_2 n_0 + \sigma/R_0. \tag{2.4}$$

The cavity profile for large values of H/b_0 is assumed to be

$$n/n_0 = \exp\{-\alpha_*(x/H)^2\}, \tag{2.5}$$

in which a value of $\alpha_* = 78{\cdot}5$ was obtained previously. From (2.4) and (2.5) the following expression is obtained

$$\frac{n_0}{H}\Big/\left\{1+\frac{2\alpha_*\sigma}{(\gamma_2-\gamma_1)H^2}\right\} = \frac{2}{K_1^2}\Big/\left\{\frac{M}{(\gamma_2-\gamma_1)Ln_0^2}\right\}, \tag{2.6}$$

in which $M = \rho_1 b_0 L V_J^2$.

3. Laboratory apparatus and experimental procedure

3.1. *Circular-jet experiments*

Circular-jet experiments were conducted in a Plexiglass basin 18 in. square and 9 in. deep; $\frac{1}{8}$ and $\frac{1}{4}$ in. diameter elliptical-approach nozzles were employed. Two combinations of liquids were utilized: oil impinging on water, and water impinging on carbon tetrachloride. The heavier liquid occupied the lower 3·5 in. of the basin in all experiments

The test nozzle was attached to a vertical-traverse point gauge on the centre-line of the basin. A small pump recirculated the lighter liquid through the apparatus. A peripheral trough at the top of the basin collected the liquid as it overflowed and delivered it to a small tank for volumetric determination of flow rate. The liquid was then returned to the pump inlet for recirculation. The flow rate was set by means of a small gate valve on the discharge side of the pump.

	Fluid combinations		
Quantity	Water–CCl_4	Oil–water	Air–water
Number of tests	97	55	179
Nozzle diameter, d_0 (in.)	$\frac{1}{8}$, $\frac{1}{4}$	$\frac{1}{8}$, $\frac{1}{4}$	$\frac{1}{4}$, $\frac{1}{2}$, $\frac{3}{4}$
Nozzle elevation, H (in.)	0·2–4·7	0·2–4·7	1·2–12
Nozzle velocity, V_J(ft./sec)	1·48–20·9	0·56–7·7	25·2–420
Nozzle Reynolds number	2150–28,200	50–340	3200–80,000

TABLE 1. Ranges of test variables for the circular jet experiments

	Fluid combinations		
Quantity	Water–CCl_4	Oil–water	Air–water
Number of tests	85	27	103
Nozzle width, b_0 (in.)	0·125 to 1·0	0·25 to 1·0	0·0625
Nozzle evaluation, H (in.)	1·0 to 7·0	1·0 to 8·0	1·2 to 7·2
Nozzle velocity, V_J (ft./sec)	0·71 to 7·9	0·69 to 3·1	67·5 to 215
Nozzle Reynolds number	2120 to 9360	165 to 300	2150 to 17,500

TABLE 2. Ranges of test variables for the plane jet experiments

Cavity depths and cavity lip-heights were measured with a vertical-traverse telescope mounted close to the test basin. Cavity diameters were measured with a probe designed to make a lateral traverse through the heavier liquid.

3.2. *Plane-jet experiments*

Plane-jet experiments were carried out in a glass tank of 6 ft. length, 2 ft. height and 2·45 in. inside width. An adjustable, circular-approach brass nozzle was constructed for these tests. The nozzle width could be varied from zero to 1·5 in. Details of the nozzle design are apparent in figure 11 (plate 1). Again, oil–water and water–carbon tetrachloride were the liquid combinations.

A centrifugal pump recirculated the lighter liquid through the apparatus. The flow rate was established with a gate valve installed at the pump outlet. A flexible tube delivered the liquid to the nozzle chamber; a small baffle plate was installed just inside the chamber to dissipate the entering jet. Two additional tubes were installed at the top of the chamber to remove entrapped air. The recirculating liquid was withdrawn through a pipe manifold from each end of the tank, passed through orifice meters and returned to the pump inlet. The meters were calibrated *in situ* for both the oil and water experiments.

Cavity depths and lip heights were measured with a vertical-traverse telescope; cavity widths were measured with a scale. The depth of the heavier liquid was about 4 in. and the lighter liquid approximately 18 in.

3.3. *Scope of the experiments*

Table 1 presents a summary of the ranges of test variables for the circular jet experiments. Table 2 gives the corresponding information for the plane jet tests. For the sake of comparison, similar ranges for the previously conducted air–water experiments are included.

	Fluid combinations		
Quantity	Water–CCl_4	Oil–water	Air–water
γ_1 (lb./ft.^{3})	62·4	53·0	0·073
γ_2 (lb./ft.^{3})	98·3	62·4	62·4
$\gamma_2-\gamma_1$ (lb./ft.^{3})	35·9	9·4	62·4
μ_1 (lb. sec/ft.^{2})	$1{\cdot}79\times10^{-5}$	$3{\cdot}87\times10^{-4}$	$3{\cdot}27\times10^{-7}$
μ_2 (lb. sec/ft.^{2})	$1{\cdot}84\times10^{-5}$	$1{\cdot}79\times10^{-5}$	$1{\cdot}98\times10^{-5}$
σ (lb./ft.)	$2{\cdot}63\times10^{-3}$	$1{\cdot}13\times10^{-3}$	$4{\cdot}95\times10^{-3}$

TABLE 3. Summary of fluid properties

Specific gravities of the oil, water, and carbon tetrachloride were measured with a hydrometer. Viscosities were determined by means of an Ostwald viscometer. Interfacial tensions were determined by the capillary-tube method. Table 3 summarizes the results of these measurements. Again, the air–water combination is included for comparison.

4. Experimental results

4.1. *Circular-jet experiments*

If the effect of interfacial tension is neglected (i.e. if $\sigma = 0$), the denominator of the left-hand member of (2.3) becomes unity. A plot of the resulting modified parameters of (2.3), i.e. n_0/H vs $M/(\gamma_2-\gamma_1)\,n_0^3$, for the oil–water experiments is presented in figure 2. Though the data points are scattered, it is noticed that the scatter is consistent according to the value of the nozzle elevation H.

If the effect of interfacial tension is now included, as indicated by (2.3), it is observed in figure 3 that a good correlation of experimental data is obtained. In this figure, the ordinate is modified by the liquid properties given in table 3, by a value of $\beta_* = 125$ obtained in the previous air–water studies, and by the value of H for the particular test. In figure 3 the dashed line refers to the results obtained in the air–water experiments.

A similar plot for the water–carbon tetrachloride experiments is presented in figure 4.

In the present circular-jet experiments the value of $(H+n_0)/d_0$ extended over the range from 8·30 to 62·8. Hence only the régime of the turbulent spreading jet was investigated.

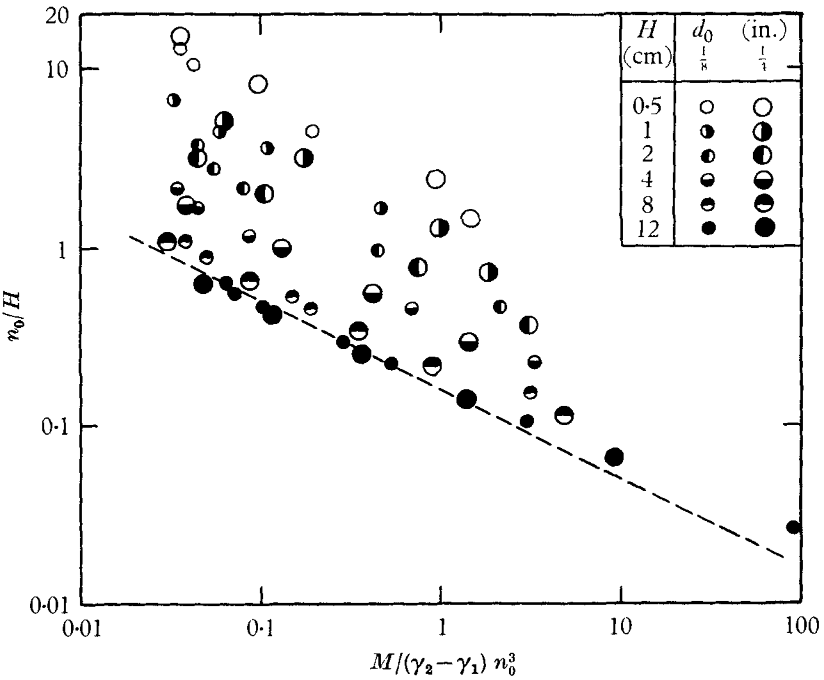

FIGURE 2. Cavity-depth data for the circular-jet oil–water experiments with the effects of interfacial tension neglected. Previously obtained air–water data are represented by dashed line.

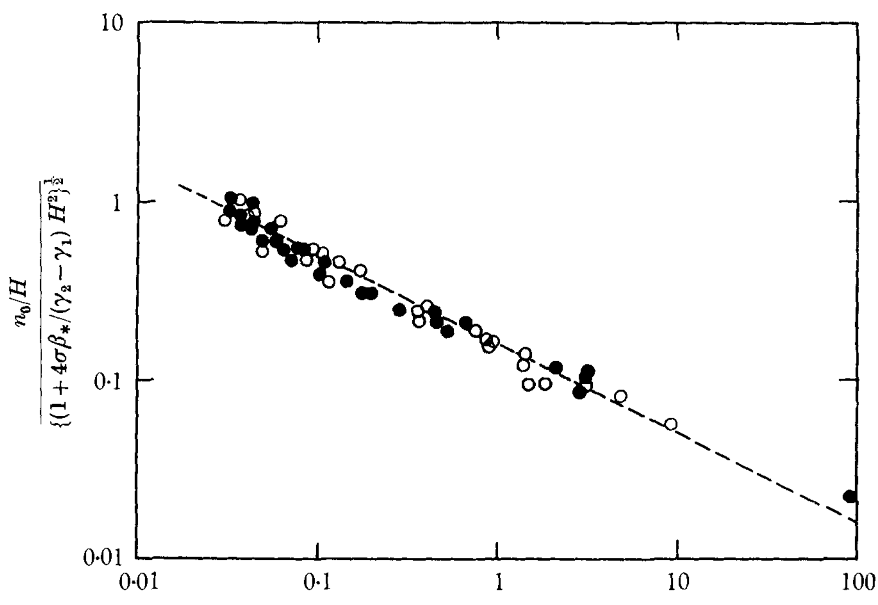

FIGURE 3. Cavity-depth data for the circular-jet oil–water experiments with the effect of interfacial tension taken into account. Nozzle diameter: ● $\frac{1}{8}$ in.; ○, $\frac{1}{4}$ in. Air–water data are represented by dashed line.

A dimensionless plot for the cavity diameters measured in the water–carbon tetrachloride tests is presented in figure 5. A cavity lip-height relationship is given in figure 6. For comparison, the dashed lines refer to the air–water experiments.

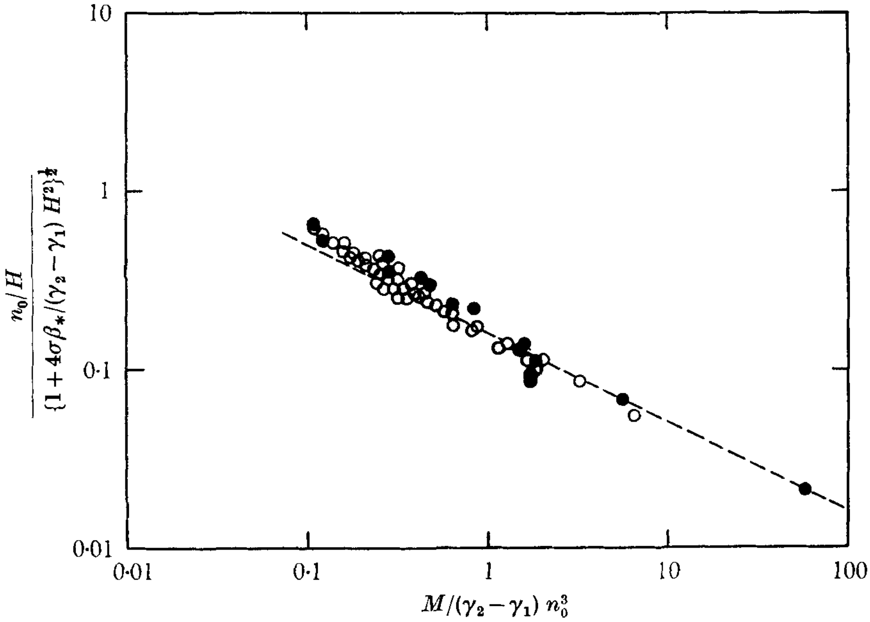

FIGURE 4. Cavity-depth data for the circular jet water–carbon tetrachloride experiments with the effect of interfacial tension taken into account. Nozzle diameter: ●, $\frac{1}{8}$ in.; ○, $\frac{1}{4}$ in. Air–water data are represented by dashed line.

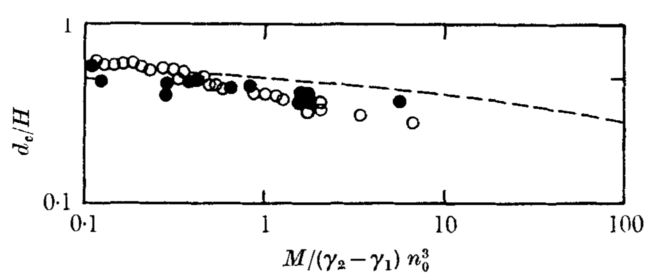

FIGURE 5. Cavity-diameter data for the circular-jet water–carbon tetrachloride experiments. Nozzle diameter: ●, $\frac{1}{8}$ in.; ○, $\frac{1}{4}$ in. Air–water data are represented by dashed line.

4.2. *Plane-jet experiments*

Cavity-depth data for the plane-jet tests are shown in figure 7; the co-ordinates for this plot are those indicated in (2.6). Not shown in figure 7 are the data points corresponding to values of $(H+n_0)/b_0$ less than eight, i.e. data associated with the régime of the free streamline jet are not included in this plot.

In the previous study, an 'added travel of jet' modification was introduced which allowed for additional jet spreading in the case of relatively deep cavities.

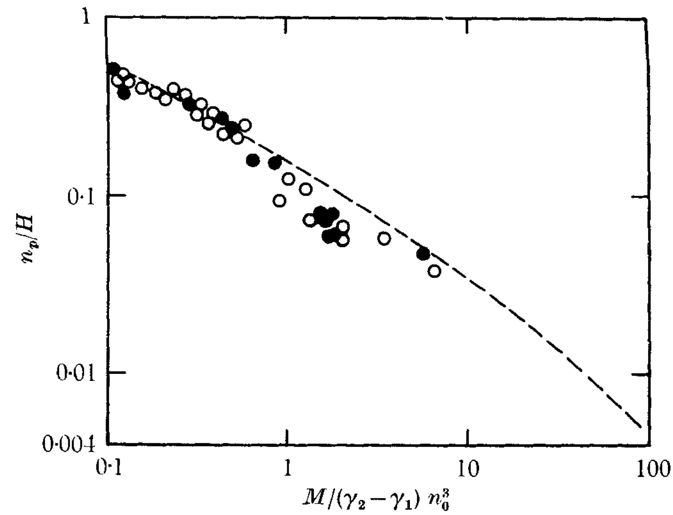

FIGURE 6. Cavity-lip height data for the circular-jet water–carbon tetrachloride experiments. Nozzle diameter: ●, $\frac{1}{8}$ in.; ○, $\frac{1}{4}$ in. Air–water data are represented by dashed line.

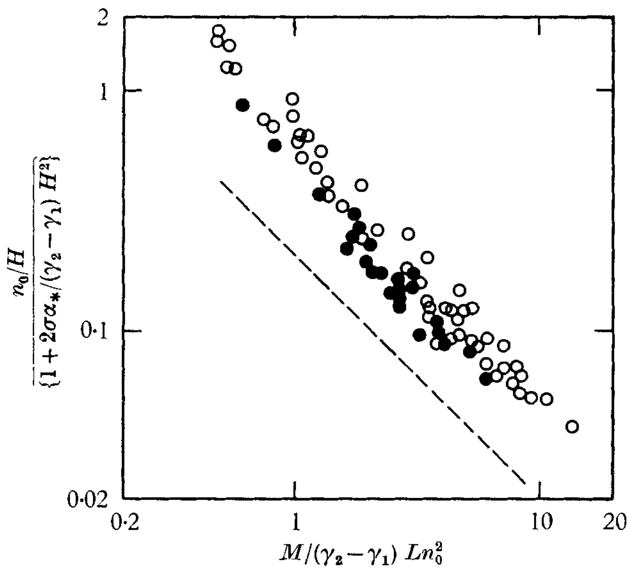

FIGURE 7. Cavity-depth data for the plane-jet experiments with the effect of interfacial tension taken into account. ●, Oil–water tests; ○, water–carbon tetrachloride tests. Air–water data are represented by dashed line.

This was manifested by substituting $H+n_0$ instead of H in the expression for the mid-plane velocity. With this modification, and if interfacial tension is neglected, then (2.6) may be written in the form

$$\frac{M}{(\gamma_2-\gamma_1)\,n_0 b_0 L} = \frac{2}{K_1^2}\left\{\frac{H+n_0}{b_0}\right\}. \tag{4.1}$$

The data for all of the plane-jet experiments, including those corresponding to low values of $(H+n_0)/b_0$ are presented in terms of (4.1) in figure 8.

Dimensional plots for cavity and cavity lip-height are given in figures 9 and 10, respectively.

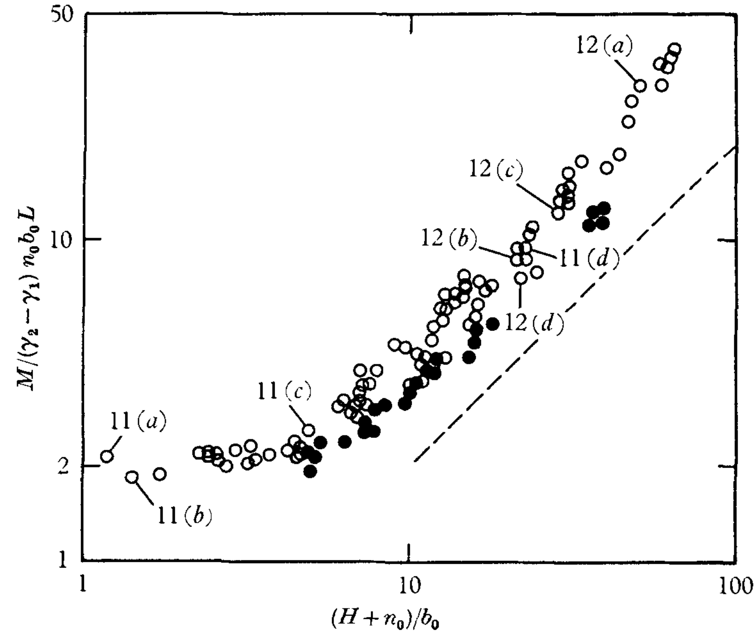

FIGURE 8. An alternative correlation of the plane-jet data, including data for the lower values of $(H+n_0)/b_0$. The identification numbers refer to the corresponding figure numbers in plates 1 and 2 and to the tabulated data of table 4. ●, Oil–water tests; ○, water–carbon tetrachloride tests. Air–water data are represented by dashed line.

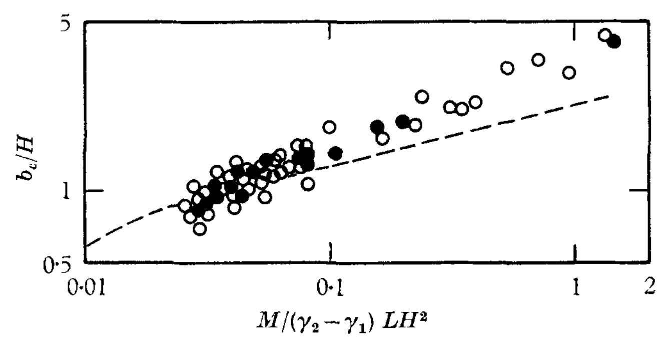

FIGURE 9. Cavity-width data for the plane-jet experiments. ●, Oil–water tests; ○, water-carbon tetrachloride tests. Air–water data are represented by dashed line.

4.3. *Description of photographs in plates* 1 *and* 2

Representative photographs of a plane water-jet impinging on carbon tetrachloride are shown in figure 11 (plate 1) and figure 12 (plate 2). Test variables associated with each photograph are given in table 4 and the corresponding data points are indicated in figure 8.

In figure 11 (*a*) and (*b*), the value of H/b_0 is such that the jet is behaving as a free streamline jet. The cavity is relatively stable and a well-defined width and lip height are apparent. Figure 11 (*c*) and (*d*) illustrate, respectively, the jet near the transition régime and in the turbulent spreading-jet régime. Again, the cavity is stable and its geometry is reasonably well defined.

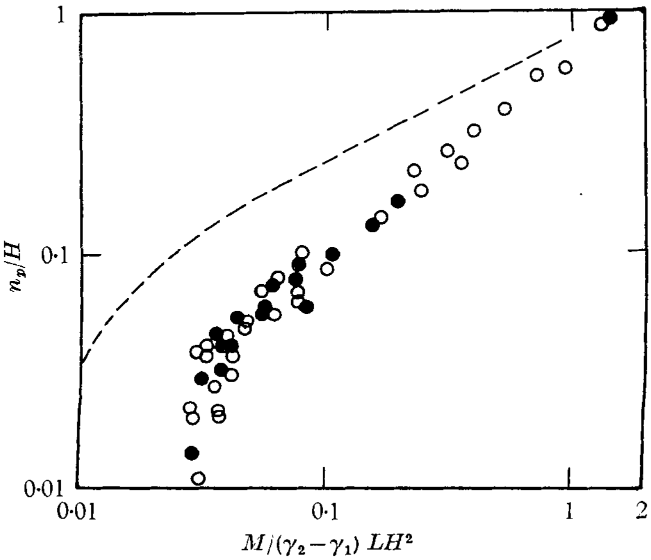

FIGURE 10. Cavity-lip height data for the plane-jet experiments. ●, Oil–water tests; ○, water–carbon tetrachloride tests. Air–water data are represented by dashed line.

Figure no.	V_J (ft./sec)	b_0 (in.)	H (in.)	n_0 (in.)	$(H+n_0)/b_0$	$M/\{(\gamma_2-\gamma_1)\,n_0 b_0 L\}$
11 (*a*)	0·79	1·0	1·0	0·19	1·19	2·12
11 (*b*)	1·12	1·0	1·0	0·43	1·43	1·88
11 (*c*)	1·29	0·5	2·0	0·41	4·82	2·61
11 (*d*)	2·98	0·25	5·0	0·61	22·3	9·35
12 (*a*)	7·86	0·125	5·0	1·32	50·6	30·10
12 (*b*)	2·86	0·125	2·0	0·62	21·0	8·50
12 (*c*)	5·36	0·125	2·0	1·53	28·2	12·10
12 (*d*)	5·13	0·51	1·0	2·27	21·8	7·52

TABLE 4. Test variables of figure 11 (plate 1) and figure 12 (plate 2)

The centre-plane velocity of the jet in the neighbourhood of the stagnation point is about 2·0 ft./sec in figure 11 (*d*). In figure 12 (*a*), this velocity is approximately 3·7 ft./sec. The difference in the appearance of the interface is very marked. In the latter, the interfacial velocity is sufficiently large to disperse the heavier liquid into the lighter. This phenomenon evidently corresponds to the 'sputtering' of water drops observed in the earlier study.

Under other conditions, the phenomenon illustrated in figure 12 (*b*) is observed. Here no significant interfacial shearing occurs but the cavity is laterally unstable. The photograph shows the cavity near its maximum excursion to the left. At a frequency of about one cycle per second, the cavity oscillates horizontally in the plane of the photograph. The length of the tank was altered by inserting false ends; this had no effect on the period of amplitude of cavity oscillation. It is possible that the proximity of the bottom or the lower face of the nozzle may have caused the cavity oscillation. This phenomenon warrants further study.

These two phenomena, i.e. interfacial shearing and cavity oscillation, may occur simultaneously, as illustrated in figure 12(*c*). Finally, as figure 12(*d*) shows, the jet can be so deeply penetrating that the interface is obliterated by an emulsion and, due to recirculation, the jet liquid is comprised of both phases.

4.4. *Discussion and conclusions*

Plots for the circular-jet-test data given in figures 3 and 4 indicate that the minus one-half power slope, anticipated by (2.3), is confirmed, at least over most of the test range. The curve constant of (2.3), $(\pi/2K_2^2)^{\frac{1}{2}}$, yields $K_2 = 7{\cdot}9$; the same value was obtained in the earlier air–water experiments.

Similarly, for the plane-jet experiments, figure 7 appears to confirm the minus-one power slope predicted by (2.6). The curve constant, $2/K_1^2$, yields a value of $K_1 = 2{\cdot}5$ for the oil–water tests and $1{\cdot}9$ for the water–carbon tetrachloride experiments. The previous air–water tests gave a value of $K_1 = 3{\cdot}17$. The reason for these discrepancies in the plane-jet experiments is not apparent. It is observed that the plane-jet data are more poorly correlated than are the circular-jet data; this was also true in the air–water experiments. Undoubtedly, the presence of the side walls is a contributing factor; the boundary layers developed by the walls may account for some of the discrepancy.

It is observed in figure 8 that the data approach the value

$$M/(\gamma_2-\gamma_1)\,n_0 b_0 L = 2$$

for small values of $(H+n_0)/b_0$. This result tends to confirm (3.8) of the previous paper.

To generalize on the main point of the present investigation, one may examine the denominator of the left-hand members of (2.3) and (2.6). These terms represent the ratio of interfacial tension to buoyancy force, i.e. the ratio of Froude number to Weber number. When this ratio is small compared to unity, interfacial tension is negligible compared to buoyancy. When the ratio is large, interfacial tension dominates the buoyancy force.

It is concluded that the analytical model provides a good framework for the analysis and presentation of experimental data. It appears that cavity depths for other gas–liquid or liquid–liquid combinations could be computed on the basis of the results obtained in the present study. An intriguing direction for further work is that associated with the interfacial-shearing and cavity-oscillation phenomena.

This investigation was carried out at the SEATO Graduate School of Engineering in Bangkok. Mr Michael Northcutt of the Voluntary Service Overseas Program and Mr Pinate Tayoongwongse are acknowledged for constructing, respectively, the plane-jet and the circular-jet test apparatus. Mr S. Parviz Sani of the University of Peshawar is acknowledged for his assistance with the circular-jet experiments. We are grateful to one of the referees of the previous paper for suggesting the present study.

REFERENCES

BANKS, R. B. 1962 *Proc. Conf. on Hydraulics and Fluid Mech.* (ed. R. SILVESTER), p. 111. Univ. of Western Australia, Nedlands. Oxford: Pergamon Press.

BANKS, R. B. & CHANDRASEKHARA, D. V. 1963 *J. Fluid Mech.* **15**, 13.

CORRSIN, S. & UBEROI, M. S. 1949 *NACA TN* no. 1865.

MAATSCH, J. 1962 *Tech. Mitt. Krupp*, **20**, 1.

OLMSTEAD, W. E. & RAYNOR, S. 1964 *J. Fluid Mech.* **19**, 561.